

Original Article

Cryopreserved allogenic fibroblast sheets: development of a promising treatment for refractory skin ulcers

Soichi Ike¹, Koji Ueno¹, Masashi Yanagihara¹, Takahiro Mizoguchi¹, Takasuke Harada¹, Kotaro Suehiro¹, Hiroshi Kurazumi¹, Ryo Suzuki¹, Tomoko Kondo², Tomoaki Murata³, Bungo Shirasawa⁴, Noriyasu Morikage¹, Kimikazu Hamano¹

¹Department of Surgery and Clinical Sciences, Yamaguchi University Graduate School of Medicine, Ube, Japan;

²Department of Molecular Pathology, Yamaguchi University Graduate School of Medicine, Ube, Japan; ³Institute of Laboratory Animals, Yamaguchi University, Ube, Japan; ⁴Department of Medical Education, Yamaguchi University Graduate School of Medicine, Ube, Japan

Received March 1, 2022; Accepted May 5, 2022; Epub June 15, 2022; Published June 30, 2022

Abstract: The purpose of this study was to investigate the therapeutic effect of cryopreserved allogenic fibroblast cell sheets in a mouse model of skin ulcers. It is necessary to reduce the cost of regenerative medicine for it to be widely used. We consider that cell sheets could be applied to various diseases if cryopreservation of allogenic cell sheets was possible. In this study, fibroblasts were frozen using a three-dimensional freezer. Freeze-thawed fibroblasts had ~80% cell viability, secreted $\geq 50\%$ vascular endothelial growth factor, hepatocyte growth factor, and stromal derived factor-1 α compared with non-frozen fibroblast sheets, and secreted approximately the same amount of transforming growth factor- β 1. There was no difference in wound-healing rates in the skin ulcer model between non-frozen and freeze-thawed fibroblast sheets regardless of autologous and allogenic cells. The degree of angiogenesis was comparable between autologous and allogenic cells. The number of CD3-positive cells in healed tissues was larger for allogenic fibroblast sheets compared with autologous fibroblast sheets. However, histopathological images showed that the fibrosis, microvascular density, and healing phase of the wound in allogenic freeze-thawed fibroblast sheets were more similar to autologous freeze-thawed fibroblast sheets than to allogenic non-frozen fibroblast sheets. These results suggest that allogenic freeze-thawed fibroblast sheets may be a promising therapeutic option for refractory skin ulcers.

Keywords: Regenerative medicine, freeze-thawed fibroblast sheet, allogeneic transplantation

Introduction

In the United States, more than 6 million people suffer from chronic ulcers caused by pressure ulcers and vascular, inflammatory, and rheumatoid subtypes, and the number of patients is expected to increase with the growing elderly and diabetic populations. The cost of treatment is too high to ignore because chronic ulcers take a long time to heal [1] and recur frequently [2]. In clinical practice, health-care workers encounter cases of refractory skin ulcers caused by arteriosclerosis obliterans, venous insufficiency, and diabetes mellitus that are non-responsive to treatment with ointments, dressings, local negative pressure closure therapy, hyperbaric oxygen treatment, and surgery [2-5]. As a result, it is important to

develop novel treatments for refractory skin ulcers.

Cell sheet technology is reported to be effective as a cell transplantation method with high cell engraftment efficiency [6]. In our previous study, we found that stem cell sheets improved cardiac function by inducing angiogenesis in the ischemic heart [7-9]. We conducted a clinical study of cell transplantation for patients with severe lower limb ischemia and frequently encountered ulcers [10, 11]. We hypothesized that the transplantation of cell sheets onto refractory skin ulcers could be used to heal them. Therefore, we conducted a study on the use of autologous cell mixed sheet transplantation in animal models of skin ulcers [12-15]. In the clinical study, we were unable to perform

cell transplantation because we could not isolate a sufficient number of high-quality cells from patient-derived tissues for transplantation [15]. Accordingly, we considered that the transplantation of allogenic cell sheets should be developed for patients who need cell sheet transplantation. In a pilot study, we transplanted autologous and allogenic fibroblast sheets in an animal model to develop allosteric cell sheet therapy for refractory skin ulcers. We found that allogenic and autologous fibroblast sheets showed the same therapeutic effect [16].

High cost is currently one of the challenges restricting the widespread use of regenerative medicine and it is necessary to reduce costs for its dissemination. Therefore, we have focused on the cryopreservation of cell sheets as a means to reduce cost. One of the strengths of allogenic cell transplantation is that cells can be pre-cultured and stored for transplantation when needed. For cryopreservation, cells are normally suspended in a cell preservation solution and either cryopreserved directly in a -80°C deep freezer or stored in a -80°C deep freezer after freezing with another device such as a program freezer. However, these methods are not suitable for freezing cell sheets that are three-dimensional (3D) structures. It has been reported that a 3D freezer, which freezes objects using cold air with a uniform temperature from all directions, may be useful for the cryopreservation of cell sheets [17]. In this study, we evaluated the function of fibroblast sheets that were stored in a -80°C deep freezer after freezing with a 3D freezer.

The purpose of this study was to examine the therapeutic effect of cryopreserved and thawed allogenic fibroblast cell sheets in an animal model of ulcers. The therapeutic effect of freeze-thawed allogenic fibroblast sheets was compared with that of non-frozen allogenic fibroblast sheets and autologous fibroblast sheets. The therapeutic effect of cell sheets was evaluated by measuring the wound healing rate in a diabetic mouse model and by histopathological examination of wounds immediately after healing. CD3-positive cells are reported to accumulate in tissues after allogenic cell sheet transplantation [16, 18]. In this study, we observed the accumulation of CD-3-positive cells as an indicator of the immunogenicity of freeze-thawed allogenic fibroblast

sheets. We found that the therapeutic effect of freeze-thawed allogenic fibroblast sheets was comparable to that of autologous fibroblast sheets. Here, we report for the first time that allogenic fibroblast sheets, frozen in a 3D freezer, exert a therapeutic effect on tissue regeneration in an animal model of ulcers.

Materials and methods

Animals

Male C3H/He and C57BL/6 mice were purchased from Japan SLC, Inc. (Shizuoka, Japan). Male green fluorescent protein (GFP)-transgenic mice (C57BL6/Tg14) were provided by Masaru Okabe (Genome Research Centre, Osaka University, Osaka, Japan) [19]. All animal procedures were approved by the Institutional Animal Care and Use Committee at Yamaguchi University (approval no.: 31-093), and the experimental methods used were conducted in accordance with the approved guidelines. This study also complied with ARRIVE guidelines. Male C57BL/6 mice were administered 55 mg/kg streptozotocin intraperitoneally for 5 consecutive days to prepare the diabetic mouse model. Mice with blood glucose levels ≥ 300 mg/dL were selected as transplant recipients.

Preparation of cell sheets

Fibroblasts were isolated from the tail skin of mice using collagenase (Fujifilm Wako Pure Chemical Corporation, Osaka, Japan) and cultured in CTSTTM AIM VTM (Thermo Fisher Scientific, Waltham, MA) and 10% fetal bovine serum (Thermo Fisher Scientific). Primary fibroblast cells were seeded in a 24-well plate (4.2×10^5 cells/well) using 2 mL medium consisting of CTSTTM AIM VTM and HFDM-1 (+) (Cell Science & Technology Institute, Miyagi, Japan) supplemented with 5% fetal bovine serum and incubated for 3 days at 37°C and 5% CO_2 . In contrast, freeze-thawed fibroblast sheets were incubated for only 1 day. After removing the culture medium from the 24-well plate, 300 μL /well STEM CELL BANKER[®] GMP grade or STEM CELL BANKER[®] DMSO-free GMP grade (ZENOAQ Resource Co., Ltd., Fukushima, Japan) was added to the wells. The plates were placed into a 3D freezer (Koga Sangyo Co., Ltd., Yamaguchi, Japan) at -35°C for 20 min to freeze the cells and then transferred to a -80°C deep

freezer. Cryopreserved cells were thawed on a Thermo Plate® (Tokai Hit Co., Ltd., Shizuoka, Japan) at 37°C for 12 min, followed by incubation for 2 days.

Histological analysis

For hematoxylin and eosin (H&E) and azocarmine aniline blue (Azan) staining as well as fluorescent immunostaining, cutaneous tissues or fibroblast sheets were collected, fixed in 10% formalin neutral buffer solution, and embedded in paraffin. Sections (thickness, 3 µm) were cut and mounted on glass slides, deparaffinized in xylene, and rehydrated in a graded ethanol series. Heat-induced antigen retrieval was performed using Target Retrieval Solution (S1699; Dako Cytomation A/S, Copenhagen, Denmark) for 30 min at 100°C and incubated with blocking buffer (X0909; Dako) for 20 min at room temperature. The following antibodies were used: anti-F4/80 (ab16911; Abcam, Cambridge, UK); anti-CD3 (ab16669; Abcam); anti-α smooth muscle actin (αSMA) (ab5694; Abcam); anti-CD31 (ab28364; Abcam); anti-GFP pAb (598; MEDICAL & BIOLOGICAL LABORATORIES CO., LTD., Aichi, Japan); purified anti-mouse MHC class II (I-A/I-E) (M5/114.15.2) (70-5321-U100; Tonbo Biosciences, San Diego, CA); goat anti-rabbit IgG H&L secondary, Alexa Fluor® 488 conjugate (ab150077; Abcam); goat anti-rabbit IgG H&L secondary, DyLight® 550 conjugate (ab96884; Abcam); and donkey anti-rat IgG H&L secondary, DyLight® 550 conjugate (ab102261; Abcam). All histological images were captured using a BZ-X710 microscope (Keyence, Osaka, Japan) and quantified using a BZ-X Analyzer (Keyence).

Cell viability

Primary fibroblast cells, at passage 2, were seeded in a 24-well plate (4.2×10^5 cells/well) and incubated for 1 h at 37°C in 5% CO₂ with 550 µL of a 1:10 mixture of Cell Count Reagent SF (Nacalai Tesque Co., Ltd., Kyoto, Japan) and medium. After incubation, 110 µL supernatant from each well ($n = 4$) was transferred to a 96-well plate and assayed at 450 nm on a 2030 ARVO X4 microplate reader (PerkinElmer, Boston, MA).

Enzyme-linked immunosorbent assay (ELISA)

ELISA was performed using ELISA kits (#MMV00, #MHG00, #MB100B, #MCX120I;

R&D Systems, Minneapolis, MN) for vascular endothelial growth factor (VEGF), hepatocyte growth factor (HGF), transforming growth factor-β1 (TGF-β1), and stromal derived factor-1α (SDF-1α) in the supernatant after the cell sheets were frozen, thawed, and then incubated for 3 days. After 1 day of incubation of the non-frozen sheets, the culture medium was changed to match the conditions of the freeze-thawed sheets. The concentration of each sample was subtracted from the concentration of cell culture medium in which no cells were cultured.

Cutaneous wound-healing model and cell sheet transplantation

Male C57BL/6 diabetic mice were anesthetized with 1.5% isoflurane via inhalation and a 6-mm full-thickness cutaneous wound was created on the dorsal skin with a biopsy punch. Male C57BL/6 mouse fibroblast sheets (autologous transplantation) and male C3H/He mouse fibroblast sheets (allogeneic transplantation) were transferred onto the wounds using Seprafilm® (Kaken Pharmaceutical Co., Ltd., Tokyo, Japan) as a carrier. In the control group, only Seprafilm® was transplanted. All ulcers were covered with ADAPTIC (#2012; Acclity, San Antonio, TX) and Derma-aid® (ALCARE, Tokyo, Japan) for the first 24 h and then with Airwall Fuwari (#MA-E050-FT; Kyowa, Osaka, Japan), and fixed with a Silkytex bandage (#11893; ALCARE). Along with a 10.5-mm diameter measurement, each wound was photographed with a digital camera on days 0, 1, 3, 5, 7, 9, 11, 13, and 15. Each photograph was normalized with the 10.5-mm diameter measurement and the wound area was measured manually by tracing the wound edge using ImageJ software (National Institutes of Health, Bethesda, MD). The wound contraction rate was calculated as: Day X = 1 - (wound area [Day X]/wound area [Day 0]).

Transplantation of GFP fibroblast sheets

Fibroblasts were isolated from the tail skin of male GFP-transgenic mice (C57BL6/Tg14). Cell sheets were prepared according to the method described above for preparing the cryopreserved cell sheets. Cell sheets were transplanted onto the dorsal wounds of male C57BL/6 diabetic mice.

Statistical analysis

Values are expressed as means \pm standard deviations. Comparisons between two groups were assessed by a two-tailed unpaired t-test. Comparisons among three groups were performed using one-way analysis of variance multiple comparisons with repeated measures and Bonferroni's adjustment. A probability value of less than 0.05 was considered to be statistically significant. All statistical analyses were performed using the Stata 16 (StataCorp, College Station, TX).

Results

Structure, survival rate, and secretion of growth factors in cryopreserved fibroblast sheets

To observe the morphology of fibroblast sheets with and without freezing, fibroblasts from C3H/He mice were frozen with and without a 3D freezer using a cell preservation solution containing dimethyl sulfoxide (DMSO). Fibroblasts were peeled from the bottom of a culture dish to make cell sheets. The diameter of normal contracting cell sheets (non-frozen fibroblast sheets) was ~ 6 mm with a thickness of 50 μm (**Figure 1A**). The diameter of freeze-thawed cell sheets with a 3D freezer was ~ 7 mm with a thickness of 40 μm (**Figure 1A**). Freeze-thawed cell sheets without a 3D freezer did not contract and they were very thin (**Figure 1A**).

Fibroblasts from C57BL/6 and C3H/He mice were frozen using cell preservation solutions with and without DMSO to analyze cell growth with and without freezing using a 3D freezer. Cell viability was $\sim 80\%$ in fibroblasts from both mouse strains frozen with a 3D freezer using a cell preservation solution containing DMSO (**Figure 1B**). Cell viability was approximately 26% and 64% in fibroblasts from C57BL/6 and C3H/He mice, respectively, frozen with a 3D freezer using a cell preservation solution without DMSO. According to the results shown in **Figure 1A** and **1B**, fibroblasts were cryopreserved in a cell preservation solution containing DMSO for subsequent experiments.

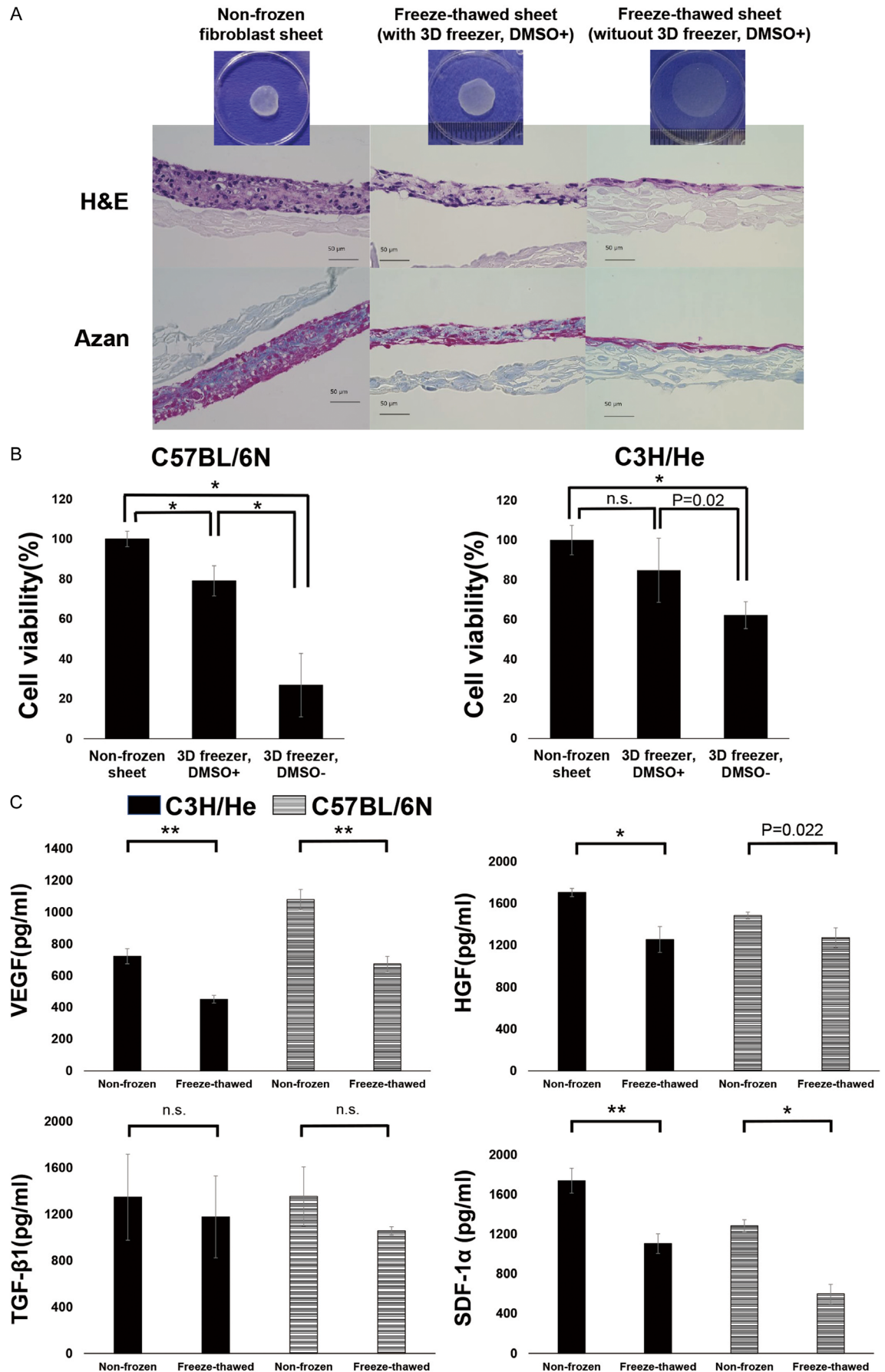
The secretion of growth factors (VEGF, HGF, TGF- $\beta 1$, and SDF-1 α) was measured in the supernatant of non-frozen cell sheets and freeze-thawed fibroblasts. Growth factor se-

cretion by freeze-thawed fibroblast sheets was 47%-86% of the level observed for non-frozen cell sheets (**Figure 1C**). To evaluate the growth factor secretion ability of cell sheets in the transplanted state, cell sheets were detached from the culture dish after preparation, cultured for an additional 3 days by changing the culture medium, and the levels of growth factors in the culture supernatant were measured. Growth factor secretion by detached freeze-thawed fibroblast sheets was 78%-85% of the level observed for detached non-frozen cell sheets (**Figure 1D**). Therefore, in the actual sheet transplantation stage, there was little difference in cytokine secretion between non-frozen and freeze-thawed sheets. Also, considering the ratio of viable cells between non-frozen and freeze-thawed sheets, viability per cell was considered to be equivalent.

Therapeutic effect of non-frozen fibroblast sheets in the cutaneous wound-healing animal model

Skin defects of 6 mm dorsal full-thickness were made using a biopsy punch in diabetic C57BL/6 mice as a cutaneous wound-healing model. Fibroblast sheets were manufactured from C57BL/6 (autologous transplantation) and C3H/He (allogenic transplantation) mice. Non-frozen fibroblast sheets were transferred onto the skin defects in the cutaneous wound-healing model to evaluate the wound-healing effect of allogeneic fibroblast sheets on days 0, 1, 3, 5, 7, 9, 11, 13, and 15 (**Figure 2A**). The wound-healing rate (%) was significantly higher in the autologous and allogeneic fibroblast sheet transplantation groups than in the control group on day 1 [allogeneic and autologous vs. control: 7.90 ± 6.62 ($P = 0.024$) and 14.34 ± 8.23 ($P = 0.002$) vs. -9.19 ± 9.96 , respectively], day 3 [allogeneic and autologous vs. control: 46.15 ± 12.67 ($P = 0.001$) and 55.06 ± 7.72 ($P < 0.001$) vs. 16.98 ± 8.69 , respectively], day 5 [allogeneic and autologous vs. control: 79.31 ± 7.14 ($P < 0.001$) and 79.86 ± 3.25 ($P < 0.001$) vs. 43.10 ± 11.85 , respectively], day 7 [allogeneic and autologous vs. control: 91.46 ± 2.28 ($P < 0.001$) and 95.03 ± 2.18 ($P < 0.001$) vs. 68.15 ± 8.44 , respectively], and day 9 [allogeneic and autologous vs. control: 99.62 ± 0.77 ($P = 0.006$) and 98.31 ± 1.57 ($P = 0.013$) vs. 87.33 ± 7.67 , respectively]. There were no significant differences among the three groups on days 11, 13, and 15 (**Figure 2B**).

Treatment for skin ulcers with cryopreserved allogenic fibroblast sheets



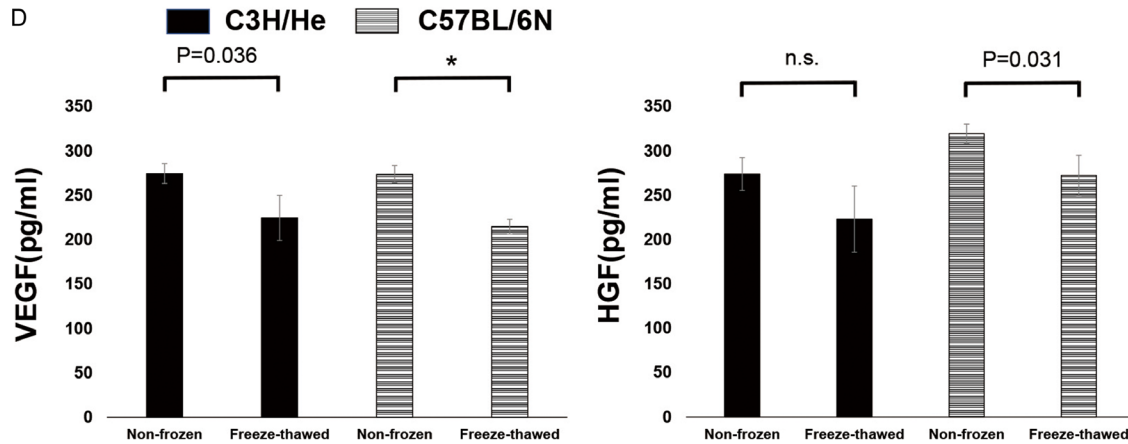


Figure 1. Histological and functional evaluation of fibroblast sheets. A. Histological observation of fibroblast sheets peeled from dishes. Non-frozen fibroblast sheet (left). Freeze-thawed fibroblast sheet with a 3D freezer (middle, thawed fibroblast sheet after freezing with a 3D freezer and storage in a -80°C deep freezer). Freeze-thawed fibroblast sheet without a 3D freezer (right, thawed fibroblast sheet after placing directly into a -80°C deep freezer). The upper images are macroscopic images of the shape and diameter of fibroblast sheets peeled from the dishes. The lower images are H&E and Azan-stained sections (Scale bars = $50\text{ }\mu\text{m}$). B. Viability of fibroblasts after freeze-thawing. Viability was evaluated using Cell Count Reagent SF at 48 h after changing the medium (non-frozen fibroblasts) or thawing (frozen fibroblasts) (C57BL/6 $n = 6, 5, 5$; C3H/He $n = 6, 5, 6$). C. Cytokine concentrations in culture supernatants of C57BL/6N or C3H/He-derived fibroblast sheets (each bar, $n = 3$). D. Cytokine concentrations in culture supernatants of C57BL/6N or C3H/He-derived fibroblast sheets that were cultured for 3 days, detached from the culture dish, the culture medium was replaced, and cultured for an additional 3 days (each bar, $n = 3$).

Therapeutic effect of freeze-thawed fibroblast sheets in the cutaneous wound-healing animal model

To evaluate the therapeutic effect of freeze-thawed fibroblast sheets, non-frozen and freeze-thawed fibroblast sheets were transplanted to the cutaneous wound-healing model (**Figure 3A**). There were no statistically significant differences in the therapeutic effect of non-frozen and freeze-thawed fibroblast sheets in autologous and allogenic transplantation on days 1 to 15 (**Figure 3B** and **3C**).

Histopathological examination of the wounds following cell sheet transplantation

H&E and Azan-stained sections were compared in all four groups (non-frozen autologous transplantation, freeze-thawed autologous transplantation, non-frozen allogenic transplantation, and freeze-thawed allogenic transplantation) on day 15. In the non-frozen autologous transplantation group, there were many mature and differentiated fibroblasts with spindle-shaped nuclei, and fibrosis had progressed. The non-frozen autologous transplantation group had a thinner epithelium than the other groups, indicating that chronic inflammation

was reduced in the wounds and the wound-healing phase had progressed. However, cell density was higher and fibrosis was less advanced in the non-frozen allogenic transplantation group compared with the non-frozen autologous transplantation group, suggesting granulation tissue. Pathologically, the wound-healing phase was delayed by several days. There were no significant differences in the histological findings between the freeze-thawed autologous and freeze-thawed allogenic transplantation groups (**Figure 4A**).

αSMA is a marker of myofibroblasts [20] and perivascular cells [21]. αSMA -positive cells were detected by fluorescent immunostaining in the wound tissue of all four groups on days 7 and 15 (**Figure 4B**). On day 7, many spindle-shaped αSMA -positive cells were found in the wounds, indicating that chronic inflammation had caused the fibroblasts to differentiate into myofibroblasts, which are involved in wound contraction. The number of spindle-shaped αSMA -positive cells was already smaller in the autologous groups compared with the allogenic groups, suggesting that tissue regeneration was slower in the allogenic groups compared with the autologous groups. On day 15, αSMA -positive cells mostly formed a luminal struc-

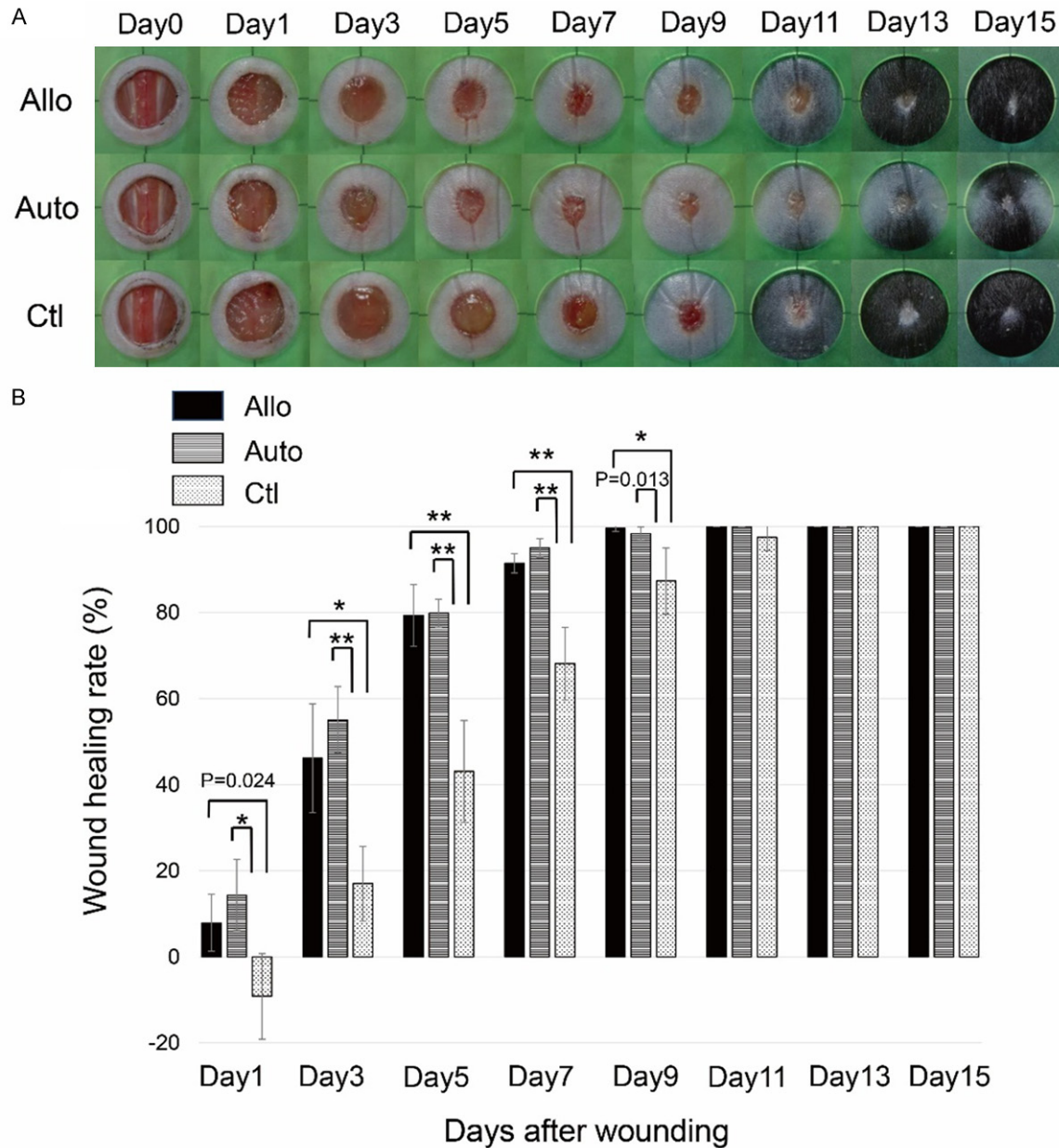


Figure 2. Therapeutic effects of non-frozen fibroblast sheets in the cutaneous wound-healing model. A. Representative macroscopic images of wounds at days 0, 1, 3, 5, 7, 9, 11, 13, and 15. Auto: non-frozen autologous transplantation ($n = 5$); Allo: non-frozen allogenic transplantation, ($n = 5$); and Control: carrier-only, control ($n = 7$). B. The wound-healing rate after fibroblast sheet transplantation was statistically compared among the three groups by day.

ture, which was thought to represent microvessels, in the non-frozen autologous, freeze-thawed autologous, and freeze-thawed allogenic transplantation groups. However, the non-frozen allogenic transplantation group had more spindle-shaped α SMA-positive cells, which appeared to be myofibroblasts, on day 15. This suggested that chronic inflammation was prolonged and the wound-healing phase was delayed in the non-frozen allogenic trans-

plantation group. To evaluate angiogenesis in tissue regeneration, CD31-positive cells were detected by fluorescent immunostaining of wound tissue in all four groups on day 15 (**Figure 4C**). There was no significant difference in microvessel density between the groups on day 15 (**Figure 4D**).

A large number of F4/80-positive cells, as macrophages, were detected by fluorescent immu-

Treatment for skin ulcers with cryopreserved allogenic fibroblast sheets

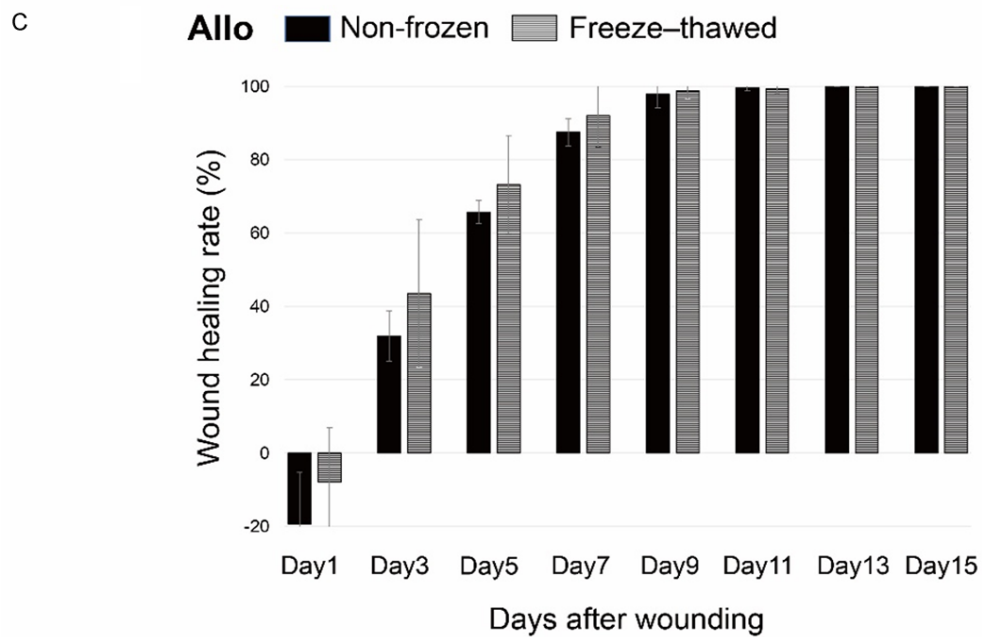
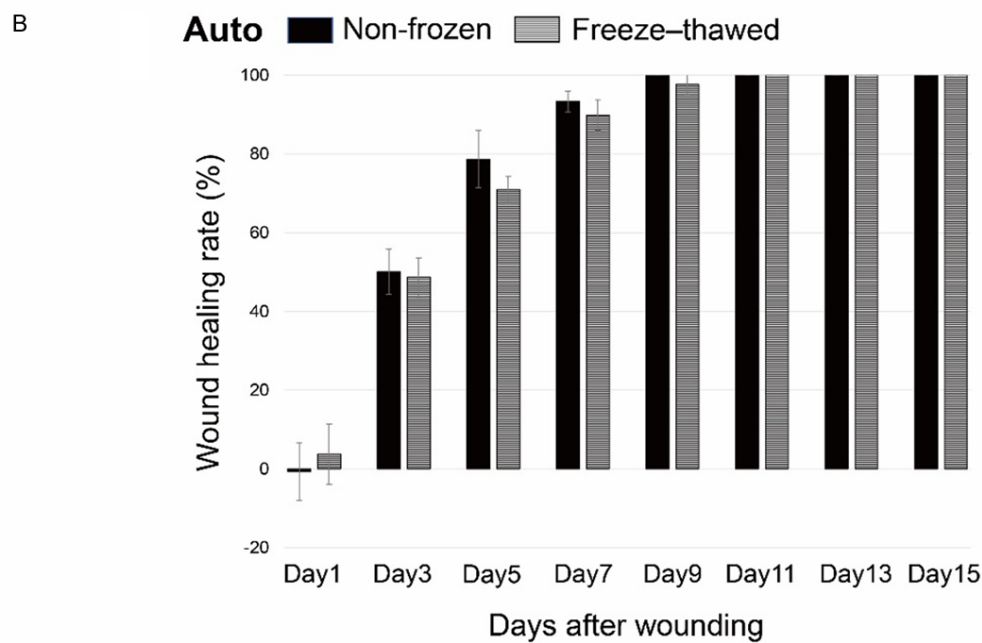
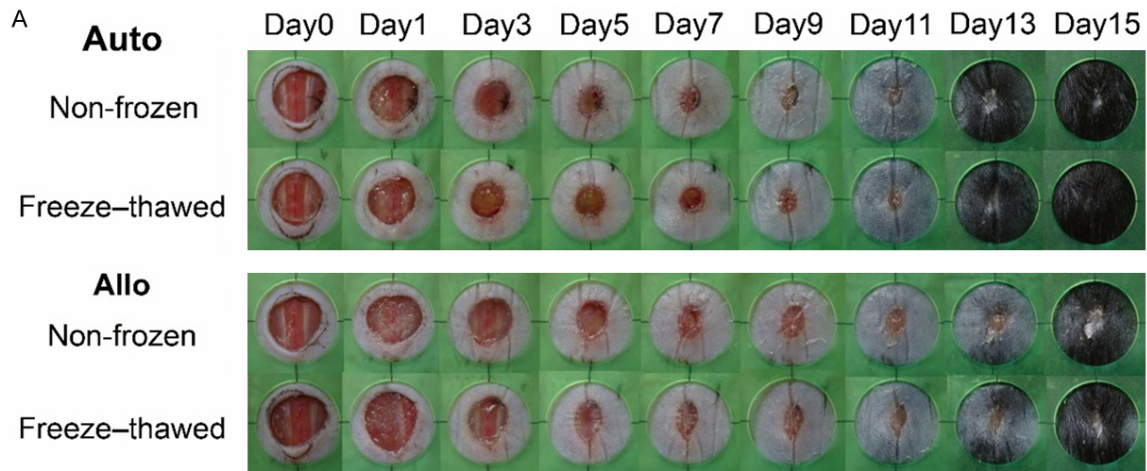


Figure 3. Therapeutic effects of freeze-thawed fibroblast sheets in the cutaneous wound-healing model. A. Representative macroscopic images of wounds at days 0, 1, 3, 5, 7, 9, 11, 13, and 15. Auto: non-frozen autologous transplantation ($n = 5$), freeze-thawed autologous transplantation ($n = 5$); Allo: non-frozen allogenic transplantation ($n = 5$), freeze-thawed allogenic transplantation ($n = 6$). B. The wound-healing rate after autologous fibroblast sheet transplantation was statistically compared between the two groups by day. C. The wound-healing rate after allogenic fibroblast sheet transplantation was statistically compared between the two groups by day.

nostaining throughout the wound tissue on day 15 (**Figure 5A**), with no significant differences in their numbers between the groups. CD3-positive cells, as T-lymphocytes, were detected by fluorescent immunostaining in wound tissue in all four groups on day 15 (**Figure 5B**). There were significantly more CD3-positive cells in the non-frozen allogenic transplantation group (198.4 ± 54.1) compared with the non-frozen autologous (55.8 ± 20.5 , $P < 0.001$) and freeze-thawed autologous (62.4 ± 18.0 , $P = 0.002$) transplantation groups (**Figure 5C**). There were also significantly more CD3-positive cells in the freeze-thawed allogenic transplantation group (152.2 ± 63.0) compared with the non-frozen autologous (55.8 ± 20.5 , $P = 0.029$) and freeze-thawed autologous (62.4 ± 18.0 , $P = 0.038$) transplantation groups (**Figure 5C**). There was no significant difference in the number of CD3-positive cells between the non-frozen and freeze-thawed allogeneic transplantation groups (**Figure 5C**).

MHC expression in fibroblasts or fibroblast sheets

Fibroblasts were isolated from the tails of male C57BL/6 GFP-transgenic mice, and GFP and MHC class II expression was analyzed in GFP-positive fibroblast sheets by fluorescent immunostaining to investigate how long the transplanted freeze-thawed fibroblast sheets remained in the cutaneous wound-healing animal model (**Figure S1**). GFP-positive fibroblast sheets expressed GFP but did not express MHC class II. The GFP-positive fibroblast sheets were freeze-thawed and transplanted to the cutaneous wound-healing model and monitored for 15 days (**Figure S2**). A GFP-positive sheet-like structure was observed until day 7 and was gradually disrupted thereafter, although GFP-positive cells were still visible. MHC class II expression was monitored until day 15 after transplanting the freeze-thawed GFP-positive fibroblast sheets. MHC class II expression was detected only in GFP-positive cells on day 1, but not after day 3 (**Figure S3**).

Discussion

Previously, we reported that monolayered cell sheets were useful material for ischemic hearts [7, 8] and ulcers [12, 13] in animal models. However, it was difficult to handle monolayered cell sheets for their clinical application. Therefore, we developed an innovative multi-layered cell sheet method and reported that transplantation of multi-layered fibroblast sheets accelerates the healing of skin ulcers [14-16] and that fibroblast sheet transplantation is useful for the prevention of postoperative complications such as bronchial apical leakage [22] and pancreatic fistula [23]. Our clinical study showed that the function of autologous cells might be reduced in a patient-dependent manner [15]. We considered that the development of allogenic cell sheets was essential for all patients who required cell sheet transplantation and reported that non-frozen allogeneic fibroblast cell sheets had the same therapeutic effect as non-frozen autologous fibroblast cell sheets in a normal mouse model of skin ulcers [16]. In the present study, the therapeutic effects of fibroblast sheets were demonstrated by employing a diabetic mouse model, which exhibits delayed wound healing, as the recipient of cell sheets (**Figure 2B**).

The cryopreservation of cell sheets will help to reduce the costs and to increase the convenience of cell sheet transplantation, which are two indispensable factors for its widespread dissemination. Two freezing methods are used in normal cell culture: slow freezing [24] and vitrification freezing [25]. We assumed that the slow freezing method was a better choice for mass production and environmental safety. Therefore, we considered that a 3D freezer might be a useful device to freeze cell sheets that have 3D structures. We previously reported that cell viability was more than 80% in freeze-thawed fibroblast sheets using a 3D freezer [17], while in the present study, it was ~80% (**Figure 1B**). Although cell viability was evaluated by intracellular metabolism using

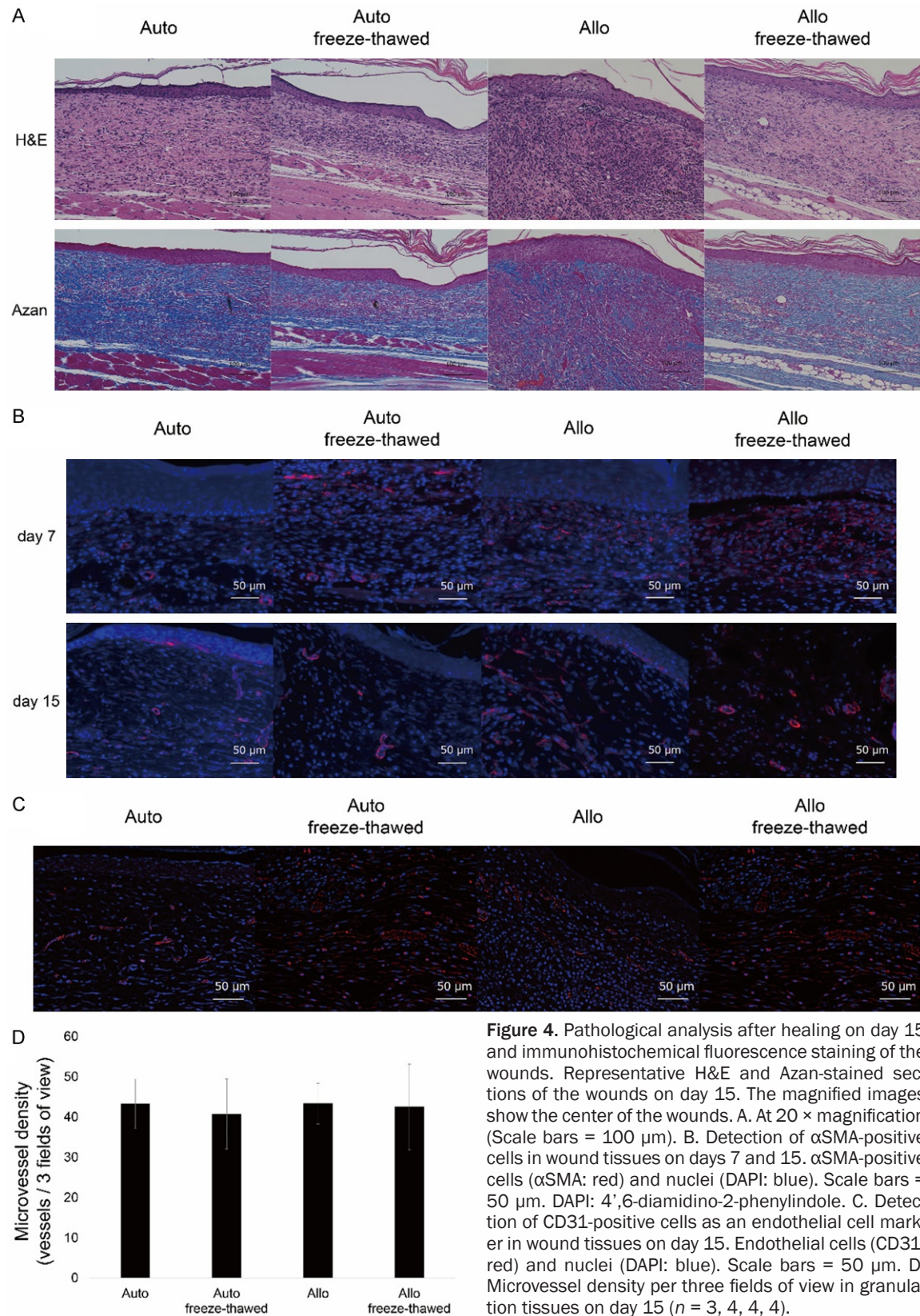


Figure 4. Pathological analysis after healing on day 15 and immunohistochemical fluorescence staining of the wounds. Representative H&E and Azan-stained sections of the wounds on day 15. The magnified images show the center of the wounds. A. At 20 × magnification (Scale bars = 100 μm). B. Detection of αSMA-positive cells in wound tissues on days 7 and 15. αSMA-positive cells (αSMA: red) and nuclei (DAPI: blue). Scale bars = 50 μm. DAPI: 4',6-diamidino-2-phenylindole. C. Detection of CD31-positive cells as an endothelial cell marker in wound tissues on day 15. Endothelial cells (CD31: red) and nuclei (DAPI: blue). Scale bars = 50 μm. D. Microvessel density per three fields of view in granulation tissues on day 15 (n = 3, 4, 4, 4).

reagents instead of cell counts because it is difficult to break down cell sheets into indi-

vidual cells, these results met the recommended criterion that cell viability should be

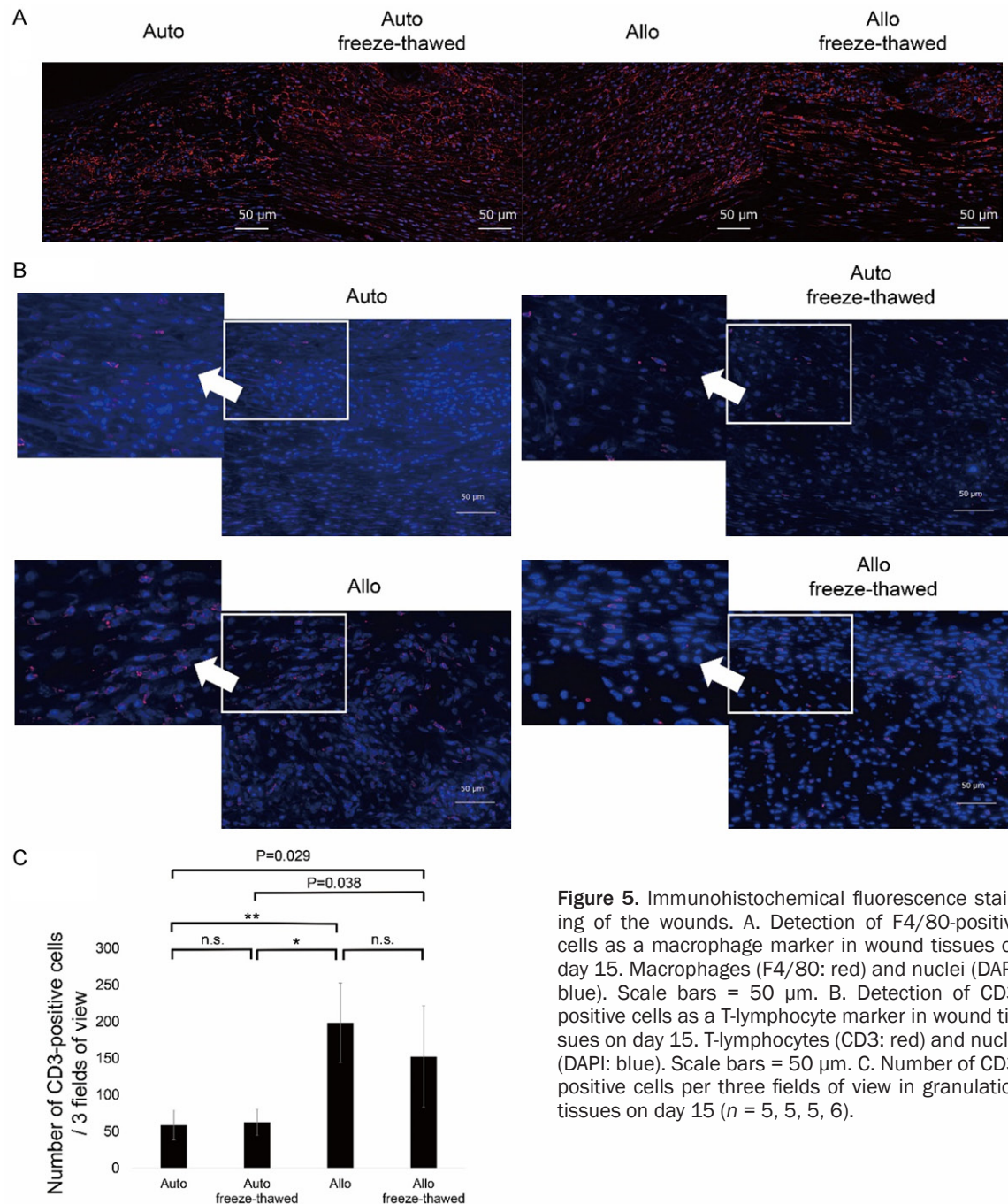


Figure 5. Immunohistochemical fluorescence staining of the wounds. A. Detection of F4/80-positive cells as a macrophage marker in wound tissues on day 15. Macrophages (F4/80: red) and nuclei (DAPI: blue). Scale bars = 50 μ m. B. Detection of CD3-positive cells as a T-lymphocyte marker in wound tissues on day 15. T-lymphocytes (CD3: red) and nuclei (DAPI: blue). Scale bars = 50 μ m. C. Number of CD3-positive cells per three fields of view in granulation tissues on day 15 ($n = 5, 5, 5, 6$).

over 70% (<https://www.fda.gov/media/73624/download>).

HGF and TGF- β 1 play important roles in the immune tolerance of allogenic mesenchymal stem cells [26]. We found that HGF and TGF- β 1 were secreted from freeze-thawed fibroblasts (Figure 1C), suggesting that they not only promote wound healing by freeze-thawed allogenic fibroblast sheets but may also temporarily

induce immune tolerance to allogenic fibroblasts in the transplanted sites. Although there was a difference in the secretion of VEGF and SDF-1 α , which promote angiogenesis, between non-frozen and freeze-thawed sheets, there was no significant difference in the number of microvessels composed of CD31-positive cells in histopathological analysis of the wounds (Figure 4D). Compared with detached fibroblast sheets, there was little difference in cyto-

kine secretion between non-frozen and freeze-thawed sheets (**Figure 1D**). In addition, considering the ratio of viable cells between non-frozen and freeze-thawed sheets, viability per cell was considered to be equivalent (**Figure 1B**). Therefore, there was no significant difference in the wound-healing rate of non-frozen and freeze-thawed sheets in both autologous and allogenic fibroblast sheets (**Figure 3B and 3C**). In the allogenic groups, although there was no significant difference in the wound-healing rate, tissue regeneration progressed more rapidly following transplantation of freeze-thawed sheets compared with non-frozen sheets because of tissue inflammation, and the number of spindle-shaped α SMA-positive cells were found to be decreased in non-frozen sheets compared with freeze-thawed sheets on day 15 (**Figure 4B and 4C**). Although there was no difference among between the non-frozen autologous and freeze-thawed autologous transplantation groups, the number of CD3-positive cells was larger in the non-frozen allogenic and freeze-thawed allogenic transplantation groups compared with the autologous fibroblast transplantation groups on day 15 (**Figure 5C**). However, tissue regeneration in the freeze-thawed allogenic transplantation group was more comparable to the freeze-thawed autologous transplantation group than to the non-frozen allogenic fibroblast transplantation group (**Figure 4A**). Normally, SDF-1 α increases neovascularization in wounds and promotes wound healing [27] and is also a potent inducer of lymphocytes, and we speculate that differences in SDF-1 α secretion may have contributed to the prolonged chronic inflammation observed in the non-frozen allogenic transplantation group. The delay in the wound healing phase due to chronic inflammation in the non-frozen allogenic transplantation group can be inferred from the high number of myofibroblasts found in the wounds (**Figure 4B**).

It is assumed that the treatment mechanism is via a paracrine effect by growth factors secreted from the transplanted cells because transplanted cell sheets disappeared from the transplant sites [12, 16] and GFP-positive fibroblast sheets were not incorporated into the healed tissue (**Figure S2**). This suggests that the period the transplanted sheets remained in the wound was almost the same between freeze-thawed autologous and allogenic fibroblast sheets because an intense immune rejection

reaction might be avoided due to the secretion of HGF and TGF- β 1 from freeze-thawed allogenic fibroblast sheets. It has been reported that mesenchymal stem cells impair their immune privilege by expressing MHC class II when transplanted into hypoxic or inflamed areas [28, 29]. Although MHC class II expression was detected in only a part of the transplanted freeze-thawed GFP-positive fibroblast sheets on day 1, it was not observed after day 3 (**Figure S3**). In addition to the immune tolerance induced by HGF and TGF- β 1, the properties without MHC class II expression prolonged the survival rate and viability of cell sheets, which may be responsible for the fact that there was no difference in wound healing rates despite differences in immune responses and the degree of chronic inflammation in the wound.

In conclusion, this study reported for the first time that freeze-thawed fibroblast sheets generated using a 3D freezer have the same therapeutic effect as non-frozen fibroblast sheets in an *in vivo* model. Thus, storing allogenic fibroblast sheets may promote the application of cell therapy by reducing its cost and increasing its convenience.

Acknowledgements

We thank Yukari Hironaka for technical assistance. This work was supported by a JSPS Grant-in-Aid for Scientific Research C (18K-08735 to B.S.) and R&D Promotion Subsidy System (Yamaguchi Prefecture Government) (to K.H.).

Disclosure of conflict of interest

None.

Address correspondence to: Dr. Koji Ueno, Department of Surgery and Clinical Sciences, Yamaguchi University Graduate School of Medicine, Minami-kogushi 1-1-1, Ube, Yamaguchi 755-8505, Japan. Tel: +81-836-22-2261; Fax: +81-836-2423; E-mail: kjueno@yamaguchi-u.ac.jp

References

- [1] Powers JG, Higham C, Broussard K and Phillips TJ. Wound healing and treating wounds: chronic wound care and management. *J Am Acad Dermatol* 2016; 74: 607-625.
- [2] Andersen JC, Leong BV, Gabel JA, Murga AG, Patel ST, Abou-Zamzam AM Jr, Teruya TH and Bianchi C. Conservative management of non-

- infected diabetic foot ulcers achieves reliable wound healing and limb salvage in the setting of mild-moderate ischemia. *Ann Vasc Surg* 2022; 82: 81-86.
- [3] Suehiro K, Morikage N, Harada T, Samura M, Takeuchi Y, Mizoguchi T and Hamano K. Self-care-based treatment using ordinary elastic bandages for venous leg ulcers. *Ann Vasc Dis* 2017; 10: 229-233.
- [4] Suehiro K, Fujita M, Morikage N, Harada T, Samura M, Suzuki R, Kurazumi H, Tsuruta R and Hamano K. Hyperbaric oxygen therapy is an effective adjunctive therapy to manage treatment-resistant venous leg ulcers. *Ann Vasc Dis* 2021; 14: 273-276.
- [5] Seidel D, Storck M, Lawall H, Wozniak G, Mauckner P, Hochlenert D, Wetzel-Roth W, Sondern K, Hahn M, Rothenaicher G, Krönert T, Zink K and Neugebauer E. Negative pressure wound therapy compared with standard moist wound care on diabetic foot ulcers in real-life clinical practice: results of the German DiaFu-RCT. *BMJ Open* 2020; 10: 1-16.
- [6] Yang J, Yamato M, Nishida K, Ohki T, Kanzaki M, Sekine H, Shimizu T and Okano T. Cell delivery in regenerative medicine: the cell sheet engineering approach. *J Control Release* 2006; 116: 193-203.
- [7] Hosoyama T, Samura M, Kudo T, Nishimoto A, Ueno K, Murata T, Ohama T, Sato K, Mikamo A, Yoshimura K, Li TS and Hamano K. Cardiosphere-derived cell sheet primed with hypoxia improves left ventricular function of chronically infarcted heart. *Am J Transl Res* 2015; 7: 2738-2751.
- [8] Tanaka Y, Shirasawa B, Takeuchi Y, Kawamura D, Nakamura T, Samura M, Nishimoto A, Ueno K, Morikage N, Hosoyama T and Hamano K. Autologous preconditioned mesenchymal stem cell sheets improve left ventricular function in a rabbit old myocardial infarction model. *Am J Transl Res* 2016; 8: 2222-2233.
- [9] Fujita A, Ueno K, Saito T, Yanagihara M, Kurazumi H, Suzuki R, Mikamo A and Hamano K. Hypoxic-conditioned cardiosphere-derived cell sheet transplantation for chronic myocardial infarction. *Eur J Cardiothorac Surg* 2019; 56: 1062-1074.
- [10] Esato K, Hamano K, Li TS, Furutani A, Seyama A, Takenaka H and Zenpo N. Neovascularization induced by autologous bone marrow cell implantation in peripheral arterial disease. *Cell Transplant* 2002; 56: 747-752.
- [11] Samura M, Hosoyama T, Takeuchi Y, Ueno K, Morikage N and Hamano K. Therapeutic strategies for cell-based neovascularization in critical limb ischemia. *J Transl Med* 2017; 15: 1-10.
- [12] Ueno K, Takeuchi Y, Samura M, Tanaka Y, Nakamura T, Nishimoto A, Murata T, Hosoyama T and Hamano K. Treatment of refractory cutaneous ulcers with mixed sheets consisting of peripheral blood mononuclear cells and fibroblasts. *Sci Rep* 2016; 6: 1-9.
- [13] Takeuchi Y, Ueno K, Mizoguchi T, Samura M, Harada T, Oga A, Murata T, Hosoyama T, Morikage N and Hamano K. Ulcer healing effect of autologous mixed sheets consisting of fibroblasts and peripheral blood mononuclear cells in rabbit ischemic hind limb. *Am J Transl Res* 2017; 9: 2340-2351.
- [14] Mizoguchi T, Ueno K, Takeuchi Y, Samura M, Suzuki R, Murata T, Hosoyama T, Morikage N and Hamano K. Treatment of cutaneous ulcers with multilayered mixed sheets of autologous fibroblasts and peripheral blood mononuclear cells. *Cell Physiol Biochem* 2018; 47: 201-211.
- [15] Mizoguchi T, Suehiro K, Ueno K, Ike S, Nagase T, Samura M, Harada T, Kurazumi H, Suzuki R, Harada K, Takami T, Morikage N and Hamano K. A pilot study using cell-mixed sheets of autologous fibroblast cells and peripheral blood mononuclear cells to treat refractory cutaneous ulcers. *Am J Transl Res* 2021; 13: 9495-9504.
- [16] Nagase T, Ueno K, Mizoguchi T, Samura M, Harada T, Suehiro K, Shirasawa B, Morikage N and Hamano K. Allogeneic fibroblast sheets accelerate cutaneous wound healing equivalent to autologous fibroblast sheets in mice. *Am J Transl Res* 2020; 12: 2652-2663.
- [17] Ueno K, Ike S, Yamamoto N, Matsuno Y, Kurazumi H, Suzuki R, Katsura S, Shirasawa B and Hamano K. Freezing of cell sheets using a 3D freezer produces high cell viability after thawing. *Biochem Biophys Rep* 2021; 28: 101169.
- [18] Kashiya N, Miyagawa S, Fukushima S, Kawamura T, Kawamura A, Yoshida S, Harada A, Watabe T, Kanai Y, Toda K, Hatazawa J and Sawa Y. Development of PET imaging to visualize activated macrophages accumulated in the transplanted iPSc-derived cardiac myocytes of allogeneic origin for detecting the immune rejection of allogeneic cell transplants in mice. *PLoS One* 2016; 11: 1-18.
- [19] Okabe M, Ikawa M, Kominami K, Nakanishi T and Nishimune Y. "Green mice" as a source of ubiquitous green cells. *FEBS Lett* 1997; 407: 313-319.
- [20] Hinz B, Mastrangelo D, Iselin CE, Chaponnier C and Gabbiani G. Mechanical tension controls granulation tissue contractile activity and myofibroblast differentiation. *Am J Pathol* 2001; 159: 1009-1020.
- [21] Crisan M, Corselli M, Chen WC and Péault B. Perivascular cells for regenerative medicine. *J Cell Mol Med* 2012; 16: 2851-2860.

- [22] Yoshimine S, Ueno K, Murakami J, Saito T, Suzuki R, Asai Y, Ikeda E, Tanaka T and Hamano K. Autologous multilayered fibroblast sheets can reinforce bronchial stump in a rat model. *Semin Thorac Cardiovasc Surg* 2022; 34: 349-358.
- [23] Iwamoto K, Saito T, Takemoto Y, Ueno K, Yanagihara M, Furuya-Kondo T, Kurazumi H, Tanaka Y, Taura Y, Harada E and Hamano K. Autologous transplantation of multilayered fibroblast sheets prevents postoperative pancreatic fistula by regulating fibrosis and angiogenesis. *Am J Transl Res* 2021; 13: 1257-1268.
- [24] Oegema TR, Deloria LB, Fedewa MM, Bischof JC and Lewis JL. A simple cryopreservation method for the maintenance of cell viability and mechanical integrity of a cultured cartilage analog. *Cryobiology* 2000; 40: 370-375.
- [25] Ohkawara H, Miyagawa S, Fukushima S, Yajima S, Saito A, Nagashima H and Sawa Y. Development of a vitrification method for preserving human myoblast cell sheets for myocardial regeneration therapy. *BMC Biotechnol* 2018; 18: 56.
- [26] Kot M, Baj-Krzyworzeka M, Szatanek R, Musiał-Wysocka A, Suda-Szczurek M and Majka M. The importance of HLA assessment in “off-the-shelf” allogeneic mesenchymal stem cells based-therapies. *Int J Mol Sci* 2019; 20: 5680.
- [27] Feng G, Hao D and Chai J. Processing of CXCL12 impedes the recruitment of endothelial progenitor cells in diabetic wound healing. *FEBS J* 2014; 281: 5054-5062.
- [28] Ilangumaran S, Finan D, La Rose J, Raine J, Silverstein A, De Sepulveda P and Rottapel R. A positive regulatory role for suppressor of cytokine signaling 1 in IFN- γ -induced MHC class II expression in fibroblasts. *J Immunol* 2002; 169: 5010-5020.
- [29] Abu-El-Rub E, Sareen N, Lester Sequiera G, Ammar HI, Yan W, ShamsEldeen AM, Rubinchik I, Moudgil M, Shokry HS, Rashed LA and Dhingra S. Hypoxia-induced increase in Sug1 leads to poor post-transplantation survival of allogeneic mesenchymal stem cells. *FASEB J* 2020; 34: 12860-12876.

Treatment for skin ulcers with cryopreserved allogenic fibroblast sheets

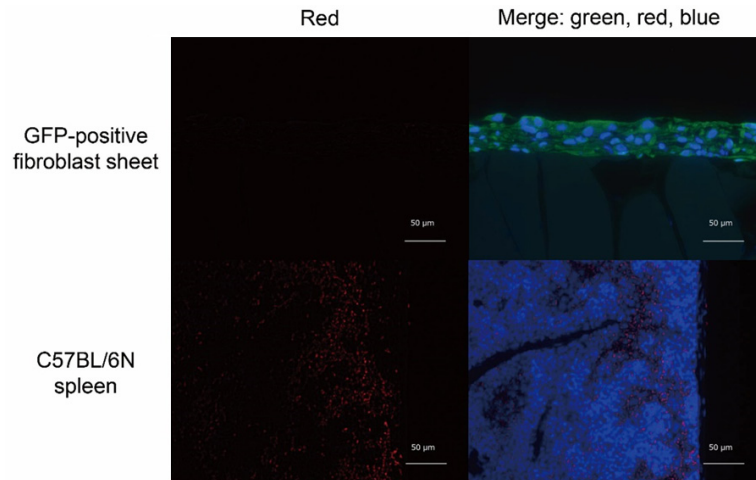


Figure S1. Observation of the period transplanted fibroblast sheets remained in the wounds and MHC class II expression with immunohistochemical fluorescence staining of skin wounds. GFP and MHC class II expression in a GFP-positive fibroblast sheet and spleen of a C57BL/6 mouse. Immunohistochemical fluorescence staining was carried out for a GFP-positive fibroblast sheet. Multicolor staining of GFP (green), MHC class II (red), and nuclei (DAPI: blue). Mouse spleen was used as a positive control for MHC class II staining.

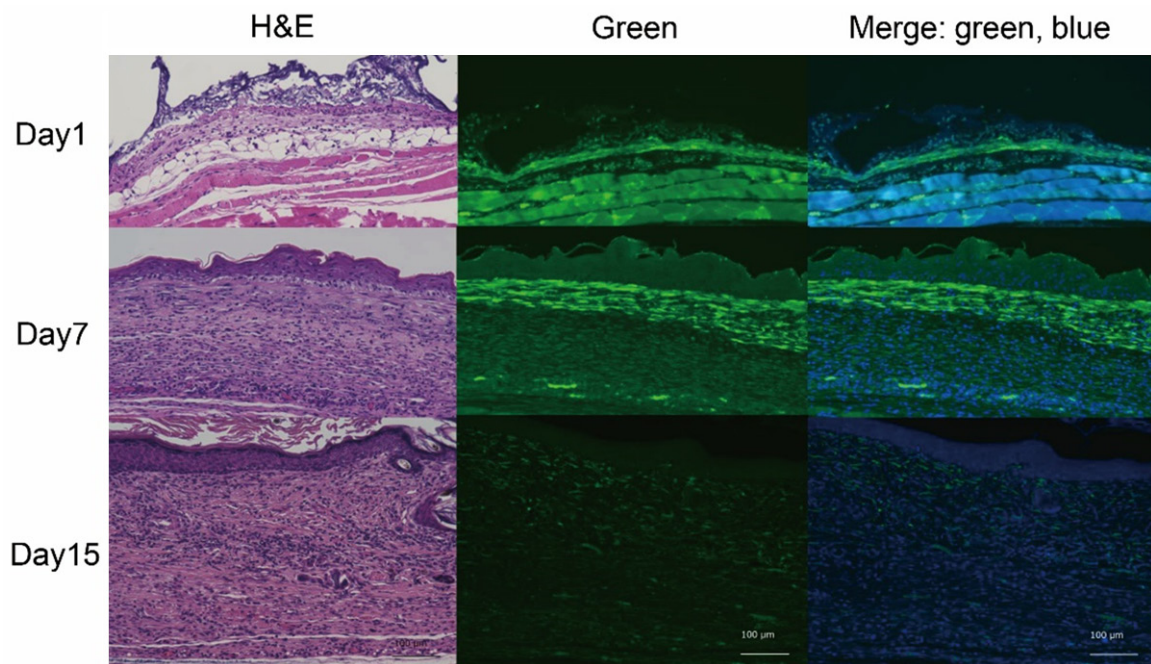


Figure S2. Detection of GFP-positive cells after transplantation of GFP-positive fibroblast sheets to the cutaneous wound-healing model. GFP-positive cells were observed over time on days 1, 7, and 15. Scale bars = 100 μm.

Treatment for skin ulcers with cryopreserved allogenic fibroblast sheets

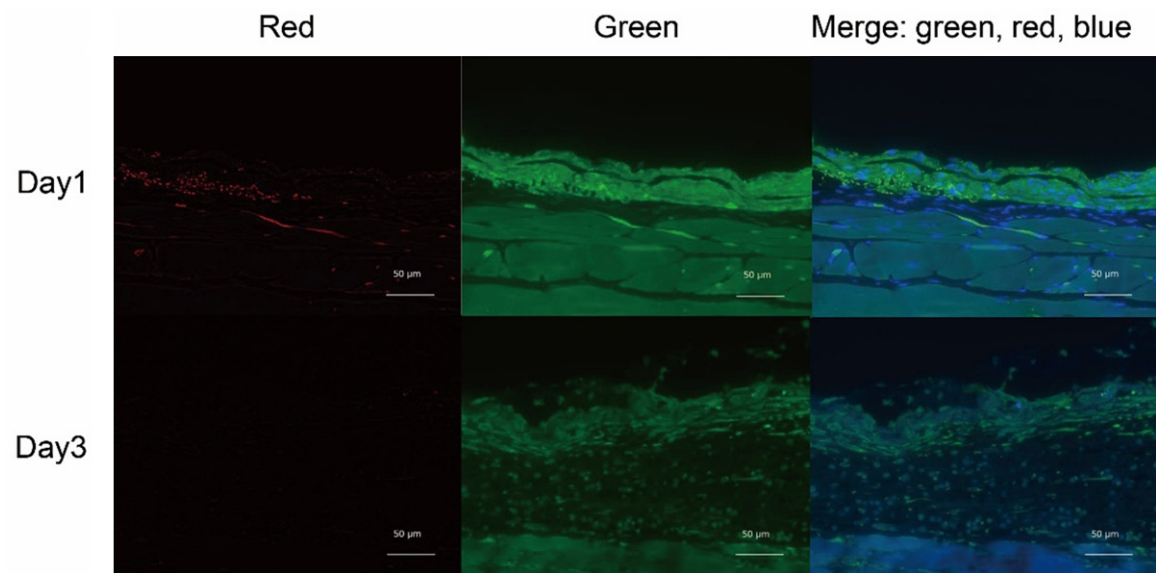


Figure S3. Detection of MHC class II expression in transplanted GFP-positive fibroblast sheets in the cutaneous wound-healing model. MHC class II expression in GFP-positive cells was observed over time on days 1 and 3. Scale bars = 50 μm .